



Review of Hydrogen Fuel Cell and Ultracapacitor Based Electric Power System Sliding Mode Control: Electric Vehicle Application

COURSE:

CONTROL OF ENERGY SYSTEMS

Omar Moukawim, 279599

Academic year:
2021-2022

Abstract: In this assignment my main goal has been to fully understand and emulate what has been done on the paper "Hydrogen Fuel Cell and Ultracapacitor Based Electric Power System Sliding Mode Control: Electric Vehicle Application" with particular attention to all the physical properties of the system.

1. Introduction

When it comes to electromobility and alternative power sources for engines, battery electric vehicles aren't the only technology that experts are expecting a lot from. Hydrogen fuel cell vehicles also present a very promising solution towards mobility without carbon emissions.

A fuel cell is a device that converts an **oxidizing agent (oxygen)** and the **chemical energy of a fuel (hydrogen)** to power an electric motor, through something called reverse electrolysis. The hydrogen comes from tanks built into the vehicle, while the oxygen comes from the ambient air. In the analyzed paper the control signals v_3 and v_4 refer respectively to the inputs of valves for Hydrogen and Oxygen. The only results of this reverse electrolysis reaction are electrical energy, heat and water, which is emitted through the exhaust as water vapor as a byproduct. So, hydrogen-powered cars are locally carbon emission-free and this is why today's early fuel cell cars and trucks can cut emissions by over 30 percent when compared with their gasoline-powered counterparts.

Refueling a fuel cell vehicle is comparable to refueling a conventional car or truck; taking less than 5 minutes to fill current models, with driving ranges of a fuel cell vehicle being similar to the ranges of gasoline or diesel-only vehicles. One of the main commercial examples is Toyota Mirai, whose 5 minutes long refilling allows to drive approximately 480 km.

Fuel cell powered vehicles can play an important role in the future thanks to their high efficiency and capability to use hydrogen as the fuel. However, they currently have some weaknesses: their cost is high and they are unable to deal with high power demands or to recuperate any braking energy. A proper implementation of a regenerative braking system could extend driving range, improve braking efficiency, reduce brake wear, and improve energy conservation. This is where **ultracapacitors** come into play to unlock hydrogen fuel cells' potential.

Ultracapacitors can serve fuel cells in a useful way: they store the energy when it is available and release it with high power when it is needed. Fuel cells in conjunction with ultracapacitors can thus create high power with fast dynamic response, which makes it well suitable for automotive applications. Ultracapacitors have proven to be a superior technology for regenerative braking in hybrid buses, trucks and trains. Hybridization of fuel cell vehicles with ultracapacitors can therefore significantly reduce the stress on fuel cells electrically and mechanically and benefit fuel economy of the vehicles. Ultracapacitors can serve high power spikes, which fuel cells alone cannot react to. As a result, adding ultracapacitors to hydrogen fuel cell vehicles can help solve some

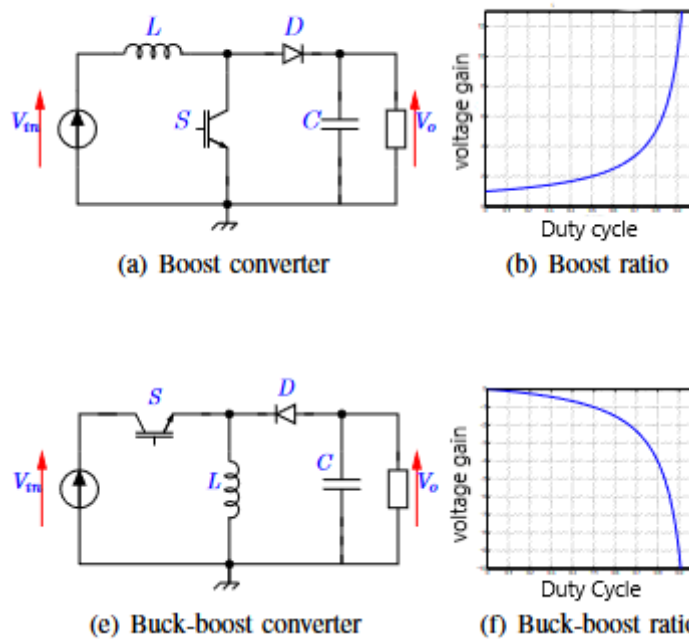
of the issues that have been preventing these vehicles from expanding.

In most stationary and mobile applications, Fuel Cells are used in conjunction with other power conditioning converters [5]. Integrating fuel cells with DC–DC boost converters provides increased, accurately regulated voltage relative to that produced by the Fuel Cell itself.

DC-DC converters are used in several applications including power supplies for personal computers, office equipment, telecommunications equipment, laptops and DC motor drives. In terms of power conversion, the above mentioned power converters play an important role in power systems using a fuel cell. The input of these converters is an unregulated DC voltage, the output is a regulated DC voltage having a magnitude (and possibly polarity) differing from the input voltage. The main characteristics required by these converters are[4]:

- High efficiency
- High power density
- Small size and low weight
- Electric isolation to prevent electric leakage and/or electric shock
- Low electromagnetic interference
- Reduced ripple current to avoid damaging the fuel cell
- Low cost

Many topologies of DC-DC converter are suitable. they can increase or decrease the magnitude of DC voltage and/or invert its polarity. In this application Boost and Buck Boost were employed, they're represented in the following figures:



In the analyzed paper the authors considered controlling the speed of an electric car in the presence of the torque disturbances and model uncertainties. This task was addressed by controlling the electric power system comprised of HFC conditioned by a DC–DC boost bidirectional power converter, with an ultra-capacitor (UC) conditioned by a boost/buck bidirectional converter, in order to drive the speed of the DC electric motor to its time varying command profile.

A remark has to be done about the type of motors employed in the paper, in fact, DC motors were considered given the fact that they have some advantages over AC motors as power drives in electric vehicles. In particular DC motors have the following advantages:

- operate with lower voltage
- have higher peak torque
- provide faster car acceleration

The main steps I have taken on to emulate the results obtained in the paper on Simulink have been the following:

1. Close reading of the paper in order to fully understand the mathematical model and all the control variables that were involved

2. Understand the idea behind the sliding mode control in order to obtain a correct implementation
3. Represent everything in Simulink in an appropriate way
4. Collection and comparison of the obtained results (wasn't possible)

1.1. Hydrogen Production, Storage, and Distribution

An obstacle to using fuel cells in vehicles is hydrogen storage. Hydrogen is produced in central processing plants where it can be produced from chemical reforming of natural gas or other fossil fuels. Fuel cell-powered vehicles must store the hydrogen in its purest form onboard as a compressed gas in pressurized tanks. It is necessary to store enough hydrogen onboard to allow vehicles to travel the same distance as fossil fuel-powered vehicles by refuelling just once every 400–450 kilometers. Due to the low-energy density of hydrogen, the volume of hydrogen required is quite substantial. Moreover, storing hydrogen in liquid form can be expensive. An alternative to storing fuel directly in the form of hydrogen is to use an onboard reformer. This is relatively costly due to the additional plant required for producing the hydrogen onboard using a reformer and the increased system complexity. Higher-density liquid fuels, such as methanol, ethanol and related bio-fuels, natural gas, liquefied petroleum gas, and gasoline, can be used for fuel, but the vehicles must have an onboard fuel reformer to reform the methanol into hydrogen. The reformer releases carbon dioxide (a greenhouse gas) increasing the carbon footprint, though less than current fossil fuel-powered engines. The use of the reformer tends to make the fuel cell power engines bulkier while also increasing the total system and maintenance costs. The hydrogen generation unit must be a compact, efficient, and low cost unit that process a fuel, such as methane, to produce hydrogen with low Carbon monoxide content which is then consumed by the fuel cell. Hydrogen production on an industrial scale is a mature technology and is based on steam reforming of low molecular weight hydrocarbon or partial oxidation of high molecular weight hydrocarbon such as methane. The partial oxidation process is sometimes substituted by autothermal reforming by adding steam and air to the methane–air mixture. The hydrogen produced by these processes is also passed through a plant for removal of carbon monoxide, desulfurization, and purification of the hydrogen. Sulfur is a poison for steam reforming nickel-based catalysts and for the platinum anode catalyst in the fuel cell and should be less than 0.001–0.1 ppm, while Carbon monoxide should be less than 5–50 ppm depending on the type of fuel cell. Desulfurization is achieved either by partial adsorption or by catalytic transformation of sulfur. Removal of Carbon monoxide is achieved in a water–gas shift unit where steam is added to convert the Carbon monoxide to carbon dioxide. Membrane reformers based on ultra-permeable Pd membranes and membrane purifiers have also developed for the purpose of reforming and purifying the fuel gas, specifically for Fuel Cells applications.

2. Mathematical model of the system

The equivalent circuit diagram of an electric power system made out of HFC/UC/DC-DC boost and boost/buck converters with a servomotor as the system's load for an electric vehicle is presented in the following picture[6]:

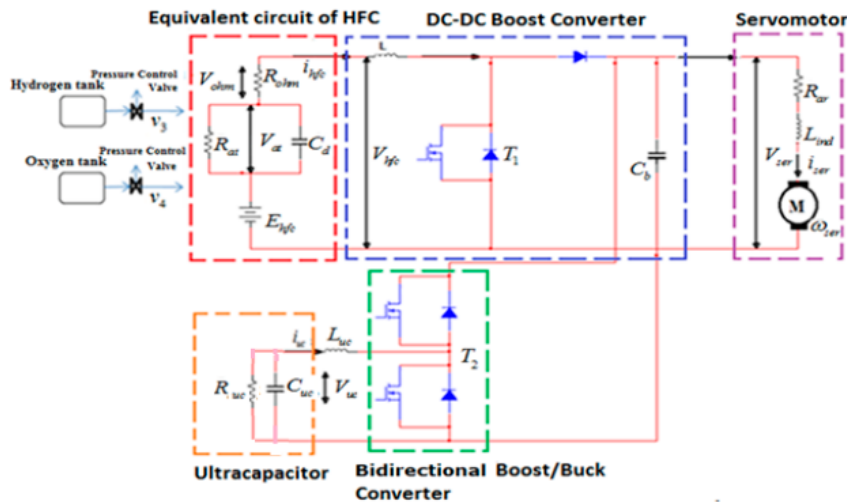


Figure 1: Complete system.

where E_{hfc} is the voltage of the HFC, i_{hfc} is the current of the HFC, V_{at} is the voltage drop across the ca-

capitance C_d due to activation loss, R_{at} is the resistance that causes this activation loss, R_{ohm} is the variable internal resistance of the HFC, V_{ohm} is the voltage drop due to ohmic losses, V_{ser} is the output voltage of the DC-DC boost converter, V_{uc} is the voltage across the capacitance C_{uc} , i_{uc} is the ultra capacitor current, R_{uc} is the resistance that characterizes the internal losses in the ultra capacitor, i_{ser} is the load (servomotor current), R_{ar} and L_{ind} are the armature resistance and inductance of the servomotor, finally, ω_{ser} is the servomotor rotational speed.

The overall mathematical system taken in consideration for the control design is the following:

$$\begin{bmatrix} \frac{dV_{ser}}{dt} \\ \frac{d^2 i_{hfc}}{dt^2} \\ \frac{di_{uc}}{dt} \\ \frac{dV_{H_2}}{dt} \end{bmatrix} = \begin{bmatrix} H_1 \\ H_2 \\ H_3 \\ H_4 \end{bmatrix} + \begin{bmatrix} -\frac{1}{C_b} i_{hfc} & 0 & -\frac{1}{C_b} i_{uc} & 0 \\ \Omega_1 & \Omega_2 & \Omega_3 & 0 \\ 0 & 0 & -\frac{1}{L_{uc}} V_{ser} & 0 \\ 0 & 0 & 0 & \frac{1}{\tau_{H_2} k_{H_2}} \end{bmatrix} \begin{bmatrix} v_1 \\ v_4 \\ v_2 \\ v_3 \end{bmatrix}$$

$$\frac{d^2 \omega_{ser}}{dt^2} = H_5 + \frac{k_m}{L_{ser}} V_{ser}$$

where

$$\begin{aligned} \Omega_1 &= \frac{1}{LC_b} \left(\frac{3}{2} i_{hfc} - i_{hfc} v_1 - i_{ser} \right); \Omega_2 = \frac{nR_g T_{st}}{4F_0 L} \left(\frac{1}{\tau_{O_2} k_{O_2} P_{O_2}} \right); \Omega_3 = -\frac{1}{C_b} i_{uc} (1 - v_1) \\ H_1 &= \frac{1}{2C_b} (i_{hfc} + i_{uc} - 2i_{ser}); H_3 = \frac{1}{2L_{uc}} (-V_{ser} + 2V_{uc}); H_4 = -\frac{1}{\tau_{H_2}} P_{H_2} - \frac{2k_{\gamma_1}}{\tau_{H_2} k_{H_2}} i_{hfc} \\ H_2 &= \frac{1}{L} \left\{ \frac{1}{2C_b} (-i_{hfc} + 2i_{ser}) + \dot{v}_1 V_{ser} - \frac{di_{hfc}}{dt} - \dot{V}_{at} + \right. \\ &\quad \left. \frac{nR_g T_{st}}{2F} \left[P_{H_2} \left(-\frac{1}{\tau_{H_2}} P_{H_2} + \frac{1}{\tau_{H_2} k_{H_2}} (v_3 - 2k_{\gamma} i_{hfc}) \right) + 2P_{O_2} \left(-\frac{1}{\tau_{O_2}} P_{O_2} - \frac{k_{\gamma_1}}{\tau_{O_2} k_{O_2}} i_{hfc} \right) \right] \right\} \\ H_5 &= \frac{1}{J} \left[-\left(\frac{k_m k_b}{L_{ind}} - \frac{b^2}{J} \right) \omega_{ser} - k_m \left(\frac{b}{J} + \frac{R_{gr}}{L_{ind}} \right) i_{ser} - n_g \left(\frac{b}{J} T_d - \dot{T}_d \right) \right] \end{aligned}$$

For the complete and correct operation of our complete Hydrogen Fuel Cell/Ultra Capacitor/Direct Current-Direct Current (HFC/UC/DC-DC) Converter/Servomotor System additional equations have to be simulated too in order to have available the full system's evolution in time and not only the evolution of the part taken in consideration for the control design, these other essential equations are the following:

$$\begin{aligned} \frac{di_{ser}}{dt} &= \frac{1}{L_{ind}} (-R_{ar} i_{ser} - k_b \omega_{ser} + V_{ser}) \\ \frac{d}{dt} P_{O_2} &= -\frac{1}{\tau_{O_2}} P_{O_2} + \frac{1}{\tau_{O_2} k_{O_2}} (q_{O_2}^{in} - k_{\gamma_1} i_{hfc}) \\ \frac{dV_{at}}{dt} &= \frac{i_{hfc}}{C_d} - \frac{V_{at}}{R_{at} C_d} \\ \frac{dV_{uc}}{dt} &= -\frac{1}{R_{uc} C_{uc}} (V_{uc} + R_{uc} i_{uc}) \\ \frac{dq_{O_2}^{in}}{dt} &= \frac{1}{\tau_{qO_2}} (-q_{O_2}^{in} + \bar{q}_{O_2}^{in}) \end{aligned}$$

All the parameters are presented in the following table:

$L_{ind} = 4 \times 10^{-3} \text{ (H)}$	$\tau_{O_2} = 6.74 \text{ (kmol/s)}$	$L = 35 \times 10^{-4} \text{ (H)}$
$k_b = 0.1 \text{ (V} \cdot \text{s} \cdot \text{rad)}$	$k_{O_2} = 2.52 \times 10^{-3} \text{ (kmol/s)}$	$L_{uc} = 140 \times 10^{-4} \text{ (H)}$
$b = 0.1 \text{ (N} \cdot \text{m} \cdot \text{s)}$	$\tau_{H_2} = 3.37 \text{ (kmol/s)}$	$R_{uc} = 1.2 \times 10^4 \text{ (}\Omega\text{)}$
$R_{ar} = 1 \text{ (}\Omega\text{)}$	$k_{H_2} = 8.49 \times 10^{-4} \text{ (kmol/s)}$	$C_{uc} = 125 \text{ (F)}$
$k_m = 5 \text{ (N} \cdot \text{m/A)}$	$\tau_{qH_2} = 2 \cdot 10^{-2} \text{ (s)}$	$T_d = 8 \sin(2t) + 10 + 2 \sin(10t) \text{ (N} \cdot \text{m)}$
$J = 0.5 \text{ (kg} \cdot \text{m}^2\text{)}$	$\tau_{qO_2} = 2 \cdot 10^{-2} \text{ (s)}$	$k_{\gamma 1} = 2.28024 \times 10^{-7} \text{ (kmol/s)}$
$n_g = 0.3$	$C_d = 68.5 \times 10^{-3} \text{ (F)}$	$R_g = 8.31417 \text{ (J/kmol)}$
$R_{at} = 0.08 \text{ (}\Omega\text{)}$	$T_{hfc} = 298.15 \text{ (K)}$	$n = 185$
$R_{ohm} = 0.06 \text{ (}\Omega\text{)}$	$T_{st} = 353 \text{ (K)}$	$\Delta G_1 = -4.4 \cdot 10^3 \text{ (J} \cdot \text{mol}^{-1}\text{)}$
$\Delta s_1 = 170.0 \text{ (J} \cdot \text{mol}^{-1} \cdot \text{K}^{-1}\text{)}$	$F_0 = 96485.3415 \text{ (s} \cdot \text{A/mol)}$	

2.1. Inconsistencies in the model

Analyzing the above mathematical model I have found out that one parameter that is required in the above Ω_3 and H_2 that is C_b is missing. I initially assumed it equal to C_d but later, after reading an older article from the same authors [1] I found it to be equal to $14 \times 10^{-3} \text{ [F]}$. Moreover in the second order derivative $\frac{d^2 \omega_{ser}(t)}{dt^2}$ there appears a never defined term \mathbf{L}_{ser} that I have assumed equal to \mathbf{L}_{ind} referring to an older paper of the same authors.

3. Control of the HFC-UC System

In the paper different control techniques were employed for different tasks, these are:

- 1-Sliding Mode Control
- 2-Sliding Mode Control
- PID

Generally the efficacy of traditional control algorithms, including a PID controller, is questionable for controlling Fuel Cell based electric power system. The problem is that a PID controller is sensitive to changes in the system parameters, such as DC load, Fuel Cell internal capacitances and inductances. The performance of a fixed-gain PID controller used for an output tracking task degrades, when the system's model has uncertain gains, and the tracking trajectory has a non-vanishing derivative. In this application it was only employed for the control of the partial hydrogen pressure \mathbf{P}_{h2} , this because its reference is considered constant $\mathbf{P}_{h2}^e = 1.01 \times 10^5 \text{ [Pa]}$ and the terms related to its control signal \mathbf{i}_{hfc} and \mathbf{P}_{h2} are measurable:

$$v_3 = k_{H_2} P_{H_2} + 2k_{\gamma 1} i_{hfc} + k_{p1} e_{4s} + k_{i1} \int e_{4s} dt$$

On the other hand, sliding mode control (SMC) is insensitive to bounded matched disturbances and plant uncertainties and is able to provide a finite time convergence of the output tracking error to zero [7]. The higher order sliding mode control (HOSM) is capable generating the continuous control while enhancing accuracy of the output stabilization [3]. This is why SMC and second order sliding mode control (2-SMC) techniques with gain adaptation were employed in the control of the Fuel Cell-Ultracapacitor based electric power system.

The challenges in controlling Hybrid Fuel Cell - Ultracapacitor that were addressed in the paper are:

1. The relatively slow dynamics of the HFC membrane challenge responding to the possible fast load current demand.
2. The non-minimum phase property of the DC-DC boost and boost/buck converters challenges a controller design that tracks a causal load voltage profile in the presence of the model perturbations.
3. The unknown bounds of the model perturbations challenge the robust controller design.

The first challenge was addressed by using a controlled Ultracapacitor as a backup of power supply whenever there is an interruption in the HFC or it is needed a fast load current demand. Fast load current is met by

splitting the current in two profiles the slow and the fast. The slow one is generated for the Fuel Cell and the fast to be followed by the Ultracapacitor.

The second challenge was tackled by controlling the Fuel Cell and Ultracapacitor currents based on the power balance condition in presence of model perturbations [1]. As soon as the non-minimum phase property of the DC-DC boost and boost/buck converters is mitigated by the Fuel Cell and Ultracapacitor control the direct tracking of the DC-DC boost and buck/boost converters is accomplished by first order sliding mode control.

The third challenge was addressed by using adaptive second order sliding mode control. Specifically, adaptive gain super-twisting controller was employed for controlling the HFC current through the partial pressure of oxygen. The servomotor speed is robustly controlled by the adaptive-gain twisting controller.

The control problem in the HFC/DC-DC/UC/servomotor electric power system is in controlling the rotational speed of the servomotor in the electric vehicle (i.e. $\omega_{ser} \rightarrow \omega_{ser}^c$). This problem reduces to design the control functions v_1, v_2, v_3, v_4 that drive the tracking errors to zero.

In particular:

- v_1 drives $e_{1s} = V_{ser}^c - V_{ser} \rightarrow 0$
- v_2 drives $e_{3s} = i_{uc}^c - i_{uc} \rightarrow 0$
- v_3 drives $e_{4s} = P_{h2}^c - P_{h2} \rightarrow 0$
- v_4 drives $e_{2s} = i_{hfc}^c - i_{hfc} \rightarrow 0$

where $V_{ser}^c, i_{uc}^c, P_{h2}^c, i_{hfc}^c$ are the command profiles.

The plan of attack on the formulated control problem was inspired by a back-stepping technique:

- Given ω_{ser}^c (for instance, it can be a command generated by an electric car driver), design the controller in terms of V_{ser} that drives $\omega_{ser} \rightarrow \omega_{ser}^c$.
- The output of this controller is considered as a command V_{ser}^c that is to be followed by the HFC/UC/DC-DC boost and boost/buck converters in the inner loop of the electric power system that generates V_{ser} . The tracking $V_{ser}^c - V_{ser} \rightarrow 0$ is enforced by the controls v_1, v_2, v_3, v_4 .

The controlled system can be schematized as follows:

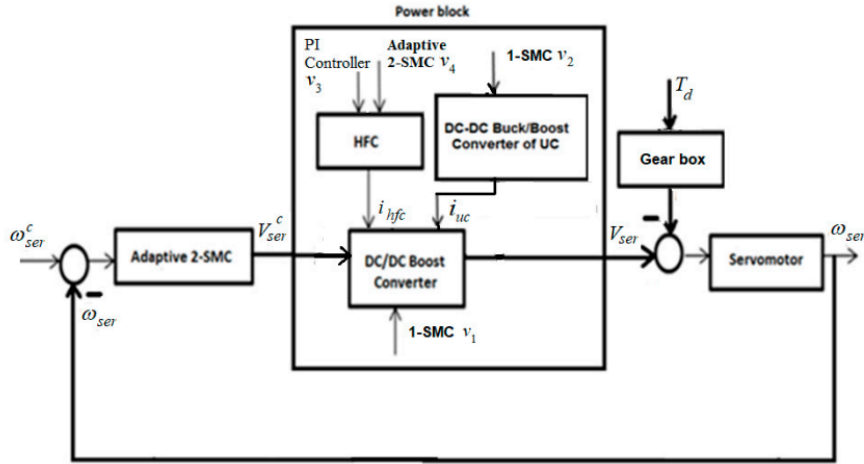


Figure 2: Complete controlled system.

3.1. HFC and UC Current Command Generator

The proposed power and current command generation management is due to the fact that the Fuel Cell dynamics are relatively slow with respect to the dynamics of the ultracapacitor [1].

The Fuel Cell current profile i_{hfc}^c , as said before, is computed based on the power balance $P_{hfc} = P_{load}$:

$$i_{hfc}^c V_{thfc} = \alpha i_{ser}^c V_{ser}^c$$

where P_{hfc} is the power generated by the Fuel Cell; P_{load} is the power consumed by the load (servomechanism); $\alpha \geq 1$ accounts for power losses (for simplicity, the power losses in the converter are neglected, and it is assumed $\alpha = 1$); i_{ser}^c is the output current command; and V_{ser}^c is the command for V_{ser} . The total voltage across n stack

of Fuel Cells is V_{thfc} .

The Fuel Cell current command profile i_{hfc}^c is computed as follows:

$$i_{hfc}^c = i_{ser}^c \frac{V_{ser}^c}{V_{thfc}}$$

The fuel cell current command i_{hfc}^c is divided into fast and slow commands and so the fast command is clearly followed by the Ultracapacitor current and the slow one by the Fuel Cell stack:

- i_{hfc} follows i_{hfc}^{cslow}
- i_{uc} follows i_{hfc}^{cfast}

So we have that i_{uc}^c is:

$$i_{uc}^c = \frac{V_{thfc}}{V_{ser}^c} (i_{hfc}^c - i_{hfc}^{cslow}) = \frac{V_{thfc}}{V_{ser}^c} i_{hfc}^{cfast}$$

Given V_{ser}^c and ω_{ser}^c the signal i_{ser}^c can be reconstructed from the following:

$$I_{ser}^c(s) = \frac{1}{L_{ind}s + R_{ar}} (-k_b \Omega_{ser}^c(s) + V_{ser}^c(s))$$

3.2. Inconsistencies in the reference generation

In the paper the constant τ referring to the division of i_{hfc} into its fast and slow component to be followed by the Fuel Cell stack and Ultracapacitor isn't provided. In my simulations I have considered it to be equal to the one employed in the reconstruction of i_{ser}^c . I have observed that in my case changing the constant τ doesn't affect that much the signal i_{hfc} so considering it equal to the Low Pass filter associated with the implementation of i_{ser}^c might be reasonable.

3.3. Sliding Mode Control

Sliding mode control is a nonlinear control technique featuring remarkable properties of accuracy, robustness, and easy tuning and implementation. Sliding mode control systems are designed to drive the system states onto a particular surface in the state space, named sliding surface. Once the sliding surface is reached, sliding mode control keeps the states on the close neighbourhood of the sliding surface. Hence the sliding mode control is a two part controller design. The first part involves the design of a sliding surface so that the sliding motion satisfies design specifications. The second is concerned with the selection of a control law that will make the switching surface attractive to the system state. There are two main advantages of sliding mode control. The first is that the dynamic behaviour of the system may be tailored by the particular choice of the sliding function. Secondly, the closed loop response becomes totally insensitive to some particular uncertainties. This principle extends to model parameter uncertainties, disturbance and non-linearity that are bounded. There are several approaches based on the sliding mode control technique:

- standard (or first-order) sliding mode control
- higher-order sliding mode control

For the first order sliding mode we have a discontinuous control, for example:

$$v_2 = 0.5 \text{sign}(e_3)$$

This can bring up some problems the main of which is *chattering*. A way to solve this problem approximate (smoothed) implementations of sliding mode control techniques have been suggested where the discontinuous "sign" term is replaced by a continuous smooth approximation, by doing some problems are attenuated but at the price of a loss of robustness. Second order sliding mode control algorithms are a powerful alternative that completely solves the chattering issue without compromising the robustness properties as well.

One popular (2-SMC) algorithm is the so called **Super-Twisting** Algorithm (control v_4 is implemented with

it), this algorithm can be seen as a nonlinear version of the classical PI controller, it is represented in the following picture:

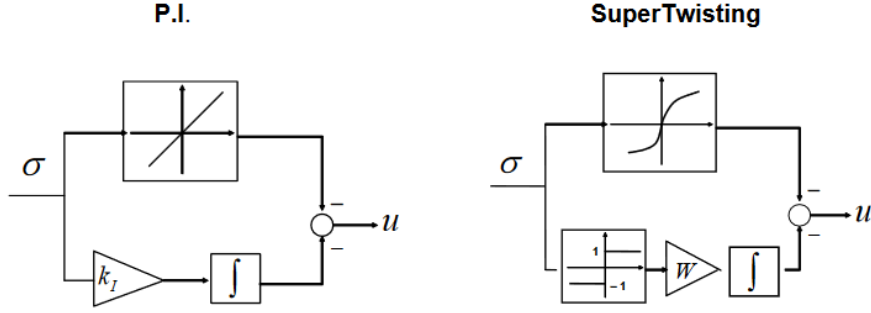


Figure 3: Bloch scheme of PI (left) and Super-Twisting (right) controllers

Second order SMC solves the chattering issue since the control law is now a continuous function of time. From a practical point of view Sliding mode control allows for controlling nonlinear processes subject to external disturbances and heavy model uncertainties. In this case the disturbance acts on the motor and is :

$$T_d(t) = 10 + 8\sin(2t) + 2\sin(10t)$$

3.4. Ultracapactor control v_2

The Ultracapacitor can be controlled in two modes:

- current i_{uc} control 1 Sliding Mode Control
- voltage V_{uc} control 2 Sliding Mode Control

I have chosen the simpler 1 Sliding more control that consists in a simple switching function:

$$v_2 = 0.5\text{sign}(e_3)$$

where the “fast” command, i_{uc}^c , for the ultra-capacitor current, i_{uc} , is generated in accordance with the discussion made in the previous section (follows the fast part of the current command i_{hfc}^c . As soon as the ultra-capacitor current i_{uc} reaches the command profile i_{uc}^c in finite time by means of the 1-SMC v_2 the error becomes $e_3 = 0$, and therefore, $i_{uc}^c = i_{uc}$ in the sliding mode.

What v_2 practically does is opening and closing the transistor T_2 in Figure [1] with a high frequency in the sliding mode, this can clearly hurt the transistor by overheating.

3.5. Control v_1 Design : 1-SMC

The control v_1 , a DC-DC converter high frequency switching control, was designed in terms of conventional 1-SMC, that is:

$$v_1 = -0.5\text{sign}(e_1)$$

What v_1 practically does is opening and closing the transistor T_1 in Figure [1].

3.6. Control v_4, v_5 2-SMC Design

The control signals v_4 and v_5 respectively control the fuel cell current i_{hfc} and the servo speed ω_{ser}^c in a continuous way. They are both proposed in terms of an *adaptive twisting control*.

Control v_4 is obtained throught the following equations:

$$v_4 = \frac{4LF_0\tau_{O_2}k_{O_2}P_{O_2}}{nR_gT_{st}}v_{4s}$$

where:

$$\begin{aligned} v_{4s} &= \alpha_{hfc} |\sigma_{2s}|^{1/2} \text{sign}(\sigma_{2s}) + v_{41s} \\ \dot{v}_{41s} &= \frac{\beta_{hfc}}{2} \text{sign}(\sigma_{2s}) \end{aligned}$$

$$\begin{aligned} \dot{\alpha}_{hfc} &= \begin{cases} \omega_h \sqrt{\frac{\gamma_h}{2}} \text{sign}(|\sigma_{2s}| - \mu_h), & \text{if } \alpha_{hfc} > \alpha_{hmin} \\ \eta_h, & \text{if } \alpha_{hfc} \leq \alpha_{hmin} \end{cases} \\ \beta_{hfc} &= 2\varepsilon_h \alpha_h, \quad \alpha_{hfc}(0) > \alpha_{hmin}, \quad \omega_h > 0 \end{aligned}$$

and the sliding surface is:

$$\sigma_{2s} = \dot{e}_{2s} + c_{2s} e_{2s}$$

On the other hand, the control v_5 is obtained from the following:

$$\begin{aligned} v_5 &= -\alpha_{ser} (\text{sign}(\sigma_{ser}) + \frac{1}{2} \text{sign}(\dot{\sigma}_{ser})) \\ \dot{\alpha}_{ser} &= \begin{cases} \omega_{1s} \sqrt{\frac{\gamma_{1s}}{2}} \text{sign}(\theta_s(\sigma_{ser}, \dot{\sigma}_{ser}) - \mu_s), & \text{if } \alpha_{ser} \geq \alpha_{sermin} \\ \chi_s, & \text{if } \alpha_{ser} < \alpha_{sermin} \end{cases} \end{aligned}$$

where:

$$\theta_s(\sigma_{ser}, \dot{\sigma}_{ser}) = \sigma_{ser}^2 + \delta_{1s} \dot{\sigma}_{ser}^2, \quad \delta_{1s} > 0$$

and the sliding surface is:

$$\sigma_{ser} = \dot{e}_{ser} + c_{ser} e_{ser}, \quad e_{ser} = \omega_{ser}^c - \omega_{ser}, \quad c_{ser} > 0$$

The servomotor speed ω_{ser} controller is finally derived in terms of the continuous output voltage command profile V_{ser}^c :

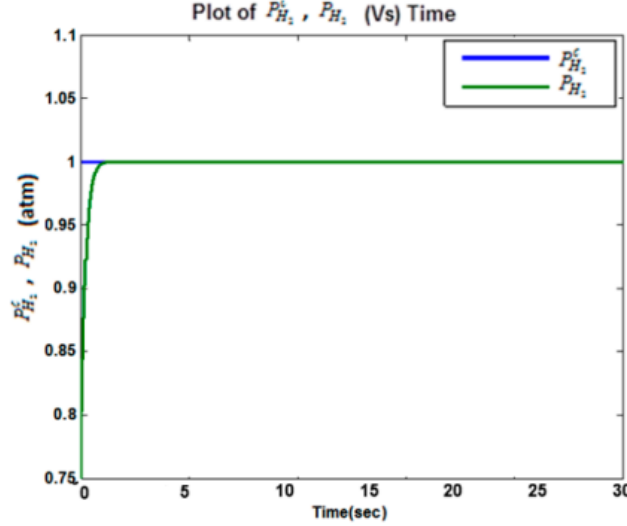
$$V_{ser}^c = \frac{L_{ser} I}{k_m} \int v_5 d\tau$$

All the parameters involved in the controller are listed in the following table:

$\alpha_{min} = 0.7$	$\mu = 0.05$	$\chi = 0.010$
$P_{H_2}^c = 1.01 \cdot 10^5 \text{ (Pa)}$	$k_{p1} = 0.45$	$k_{i1} = 1.56$
$c_2^\# = 7.5$	$\alpha_{hmin} = 1$	$\alpha_{hfc}(0) = 10$
$\omega_h = 60$	$\gamma_h = 10$	$\mu_h = 0.04$
$\varepsilon_h = 0.03$	$\eta_h = 0.01$	$\omega_{1s} = 30$
$\chi_s = 0.01$	$\mu_s = 0.08$	$\alpha_{sermin} = 0.7$
$\gamma_{1s} = 20$	$\alpha_{ser}(0) = 3$	$\delta_{1s} = 10$

3.7. Inconsistencies in the control

Throughout the paper many inconsistencies regarding unit measurements have been encountered between the values needed in the simulation and the ones actually in the presented table, an example is the target hydrogen pressure $P_{h_2}^c = 1.01 \times 10^5$ [Pa] while on the actual simulation it has to be considered of 1 [atm] as in the following plot:



Another remark regards the initial conditions, these are never mentioned in the paper and they have to be extrapolated from the results section where all the final plots are illustrated. Lastly some parameters were missing regarding the control signals v_4 and v_5 these are respectively c_{2s} and c_{ser} that are only assumed greater than zero in the paper.

4. Simulation

4.1. Approaches taken for the simulation

During the analysis of this paper I have tried different techniques of simulation in Simulink in order to try and obtain the results presented by the authors. These are:

- Simulation of the systems dynamics taken in consideration for the control and all the other dynamics needed for the validation of the results.
- Simulation of the error dynamics associated to the overall system by side of the equations in the previous point.

Regarding the Control and Reference signals I have implemented each of them in its own Matlab function, this paying high attention in order to avoid any algebraic loops. The overall system was simulated using the Euler method with a fixed step of $\Delta(t) = 10^{-4}$ [s].

5. Conclusions

After reporting each of the necessary equation on Simulink and correctly setting up Integrators Low pass filters and all the components involved in each of the approaches presented in the previous chapter (and after having checked up the equations many and many times for typos) I wasn't able to successfully recreate the results proposed by the authors. In my opinion this might all come back to the discussed inconsistencies in both the model and the control and the fact that initial conditions aren't specified in the paper. I have done the simulation all over many times changing the simulation disposition of the blocks, the most significant are:

- Simulation of the abovementioned overall system and computation of the error as a difference between the respective state variable and each command profile.
- Simulation of the actual error dynamics provided in the reference paper.

Both of the mentioned options had similar results that were quite different from the reviewed paper one. In the simulation references were created in a separate dedicated Matlab function.

From a personal point of view working on this article and its simulation has been very interesting and fun, it has allowed me to further deepen my knowledge about the Simulink environment and more importantly it gave me the opportunity to take a first look into the control of Electric vehicles domain. This field has from always been of my great interest and now I am even more aware about its complexity, mainly given by all the components involved (Fuel Cells, Ultracapacitors, DC-DC Converters ecc.). On top of that I have for the first time read about the Sliding Mode Control which hopefully I will get to understand better during my Master's studies.

For sure I have found many difficulties during the process and many seemed at first unsolvable but after looking up some reference paper or meeting up with the professors everything looked much more clear. Overall it was quite a hard task but it was definitely worth it.

6. Future Works

Super-twisting and twisting control algorithms are sensitive to unmodeled dynamics of the actuator in Equations and that can cause self-sustained oscillations of finite frequency and amplitude [2]. The effects of unmodeled dynamics of the actuator in the studied hydrogen fuel cell-based electric power system of an electric car might be investigated analytically in future work.

References

- [1] Roshini Ashok and Yuri Shtessel. Control of fuel cell-based electric power system using adaptive sliding mode control and observation techniques. *Journal of the Franklin Institute*, 352(11):4911–4934, 2015.
- [2] I. Boiko and L. Fridman. Analysis of chattering in continuous sliding-mode controllers. *IEEE Transactions on Automatic Control*, 50(9):1442–1446, 2005.
- [3] Igor Boiko. Discontinuous control systems. frequency-domain analysis and design. *Discontinuous Control Systems: Frequency-Domain Analysis and Design*, 01 2009.
- [4] Mohammad Kabalo, Benjamin Blunier, David Bouquain, and Abdellatif Miraoui. State-of-the-art of dc-dc converters for fuel cell vehicles. In *2010 IEEE Vehicle Power and Propulsion Conference*, pages 1–6, 2010.
- [5] Cristian Kunusch, Paul Puleston, and Miguel Mayosky. *Sliding-Mode control of PEM fuel cells*. Springer Science & Business Media, 2012.
- [6] Yuri B. Shtessel, Malek Ghanes, and Roshini S. Ashok. Hydrogen fuel cell and ultracapacitor based electric power system sliding mode control: Electric vehicle application. *Energies*, 13(11), 2020.
- [7] S. K. SPURGEON and R. DAVIES. A nonlinear control strategy for robust sliding mode performance in the presence of unmatched uncertainty. *International Journal of Control*, 57(5):1107–1123, 1993.